J Mater Sci (2011) 46:1581–1584
DOI 10.1007/s10853-010-4965-7

Structure and ferroelectric properties of stoichiometric and Sr-deficient–$SrBi_4Ti_4O_{15}$ thin films

Hui Sun · Xiao-bing Chen

Received: 21 May 2010 / Accepted: 29 September 2010 / Published online: 14 October 2010

Abstract $SrBi_4Ti_4O_{15}$ (SBTi) and Bi-excess and Sr-deficient SBTi (Sr-deficient SBTi, $Sr_{0.8}Bi_{4.13}Ti_4O_{15}$) thin films were deposited on Pt/Ti/SiO_2/Si (100) substrates using a sol–gel method. Structure and electric properties were investigated systematically. These films were random oriented. The remnant polarization ($2P_r$) of SBTi film was about 25.3 μC/cm^2, which was larger than the reported value of SBTi thin film. The film with Sr-deficient and Bi-excess composition showed a very large remnant polarization of 36.6 μC/cm^2. The capacitance–voltage (C–V) characteristics of both the films showed normal ferroelectric behavior. The Curie temperatures of the same Sr-deficient and Bi-excess component ceramics sample increased slightly in comparison with that of SBTi. More importantly, the Sr-deficient and Bi-excess SBTi thin film showed high fatigue resistance against continuous switching up to 4.4×10^{10} cycles.

Introduction

Ferroelectric thin films have been extensively investigated for the application in nonvolatile ferroelectric random access memories (FeRAMs) [1, 2]. For such application it is generally required that ferroelectric films have a large remnant polarization and a low coercive voltage. In addition, good endurance of polarization fatigue, the reduction in the switchable polarization after repeated switching cycles, is another requirement. Bismuth layer-structured ferroelectric (BLSF) materials are promising candidates for lead-free ferroelectric materials [1]. Among BLSFs, thin films of $SrBi_2Ta_2O_9$ (SBT) and $Bi_4Ti_3O_{12}$ (BIT) have been intensively investigated in recent years. SBT and BIT have both merits and demerits for practical applications to FeRAMs. In the case of SBT, it shows low coercive field, low leakage and excellent fatigue endurance even when in the form of thin films with Pt electrodes [1, 3, 4]. However, the remnant polarization ($2P_r$) of SBT is not sufficient for the high-density integration of FeRAMs. Noguchi et al. [4] reported that the remnant polarization of the thin films with Sr-deficient and Bi-excess composition, $Sr_{0.8}Bi_{2.2}Ta_2O_9$, is twofold that of stoichiometric SBT, and this improvement in thin films has been confirmed by several groups [3, 5]. As for BIT, although parent BIT single crystal possesses a large spontaneous polarization ($\sim$50 μC/cm^2) superior to that of SBT, devices in thin film form often suffer from high leakage current and domain pinning, leading to a much reduced polarization value ($\sim$10 μC/cm^2) [6, 7].

$SrBi_4Ti_4O_{15}$ (SBTi), another typical BLSF, possesses a more perovskite unit sandwiched between the two Bi–O layers and exhibit typical ferroelectric behavior with $2P_r$ of 58 μC/cm^2 in *a*/*b* axis orientations under an applied electric field of 60 kV/cm [8]. Importantly, SBTi has good fatigue-free property. As reported, the SBTi thin films synthesized by pulsed-laser deposition (PLD) exhibited little fatigue at least up to 10^{11} cycles on Pt electrodes [9, 10]. Considering that the $2P_r$ of SBTi thin film synthesized by other method is rather small, only $\sim$6.2–13.0 μC/cm^2 [9–12], it is worth of trying different methods to obtain films with higher remnant polarization for achieving high-density memory. In this work, sol–gel method is considered to fabricate the SBTi thin films. To enlarge the $2P_r$, Sr-deficient and Bi-excess SBTi ($Sr_{0.8}Bi_{4.13}Ti_4O_{15}$) thin film was also prepared.

H. Sun · X. Chen (✉)
College of Physics Science and Technology,
Yangzhou University, Yangzhou 225002, China
e-mail: xbchen@yzu.edu.cn

Experiments

Both stoichiometric and Sr-deficient SBTi thin films were deposited on Pt/Ti/SiO_2/Si (100) substrates using a sol–gel method. Bismuth acetate, strontium acetate, and titanium *n*-butoxide were used as precursor materials. Acetic acid and *n*-propanol were used as solvents. 5 mol% Bi-excess was added to compensate for the volatilization of Bi in the annealing process. Acetyl acetone was used as the chelating agent and ethanolamine was added to control the pH value which is kept in 3–4. The final concentration was about 0.1 mol/L. In the first step for preparing the films, the solutions were spin-coated at a speed of 3500 rpm for 30 s followed by a drying process at 200 °C for 2 min and a pyrolysis process at 400 °C for 2 min. In the second step, the films were annealed at 750 °C for 10 min in flowing oxygen atmosphere. These two steps were repeated several times to obtain a desired thickness of the films. At last, the films were then annealed at 750 °C for 30 min in oxygen for full crystallization.

To measure the electric properties, Pt dot with the area of 3.14×10^{-4} cm^2 were sputtered on the surfaces of the films as top electrodes through a shadow mask. A postannealing procedure was then followed at 600 °C for 10 min in oxygen ambient. Meanwhile, the stoichiometric and Sr-deficient and Bi-excess SBTi ($Sr_{0.8}Bi_{4.13}Ti_4O_{15}$) ceramics were prepared by the standard solid-state reaction method. The crystal structures of the films were analyzed by X-ray diffractometer (M03XHF22) with Cu K_α radiation. The surface morphology was investigated by a scanning electron microscope (SEM: XL-30ESEM). The ferroelectric properties were evaluated using a Radiant Technology RT66A and RT6000HVS Standard Ferroelectric Test Units. The capacitance–voltage characteristics of both the films were measured in the MFM configuration using a small ac signal of 10 mV at 100 kHz by HP-4192A low-frequency impedance analyzer. The Curie temperatures of both ceramics were determined from the dielectric permittivity (ε) measurement with HP-4192A. Pellet for dielectric property measurement has a typical thickness of 0.7 mm and the electrode diameter of 2.0 mm.

Results and discussions

Figure 1 represents the XRD θ–2θ scan of stoichiometric and Sr-deficient SBTi thin films annealed at 750 °C. Both the films are well crystallized and possess a BLSF ferroelectrics crystal structure. The coincident peaks of the SBTi and the Sr-deficient SBTi thin films indicate that the composition with Sr-deficient and Bi-excess does not affect the basic crystal structure of SBTi. As is shown, both the films are random oriented. For SBTi, the strongest peak is

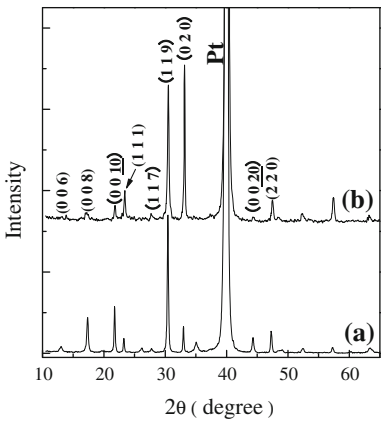

Fig. 1 XRD pattern of the **a** SBTi and **b** Sr-deficient SBTi thin films

the (1 1 9), whereas, the most prominent peak is the (0 2 0) for Sr-deficient SBTi film, which is suggesting that composition with Sr-deficient and Bi-excess increase the *b*-orientation of the film.

Figure 2 illustrates typical surface images of (a) SBTi and (b) Sr-deficient SBTi films scanned by SEM. Both films are composed of rod-like grains with seldom flake grains. According to Do et al. [13], the shape of the grain is related to the crystallographic orientation of the BLSFs, and the rod-like grains match to either (1 1 9) or *a*-axis orientation in SBTi thin films. Furthermore, most of the grains parallel to the substrate plane. All these are in accordance with the XRD results. It also can be seen that Sr-deficiency doses not change the grain shape but decrease the size of the grains.

The polarization–electric field (*P*–*E*) properties of the stoichiometric and Sr-deficient SBTi thin films are depicted in Fig. 3. Under the electric field of 324 kV/cm, both of the samples exhibit well-saturated hysteresis loops. For SBTi, $2P_r$ reaches the value of 25.3 μC/cm^2, which is remarkably higher than the PLD-grown and MOD-grown SBTi thin films [8–10, 13, 14]. Note that the composition with Sr-deficient and Bi-excess results in a very large $2P_r$ of 36.6 μC/cm^2, which is increased by nearly 45% in comparison with that of SBTi.

The larger $2P_r$ value of SBTi compared to those films derived from PLD and MOD method might be attributed to several causes: one is the larger grain size. Ren et al. [15, 16] reported a transmission electron microscopy study on $PbTiO_3$ thin films that domain wall in small grains were very stable under an external field, while domains in large grains were easier to switch. The other is the effect of grain orientation in the thin film. Since spontaneous polarization along *c*-axis is much smaller than those along *a* (*b*) axis [8], the less *c*-axis oriented SBTi thin film would induce larger polarization. Besides, it is also related to our process conditions, such as well-balanced hydrolyzation and

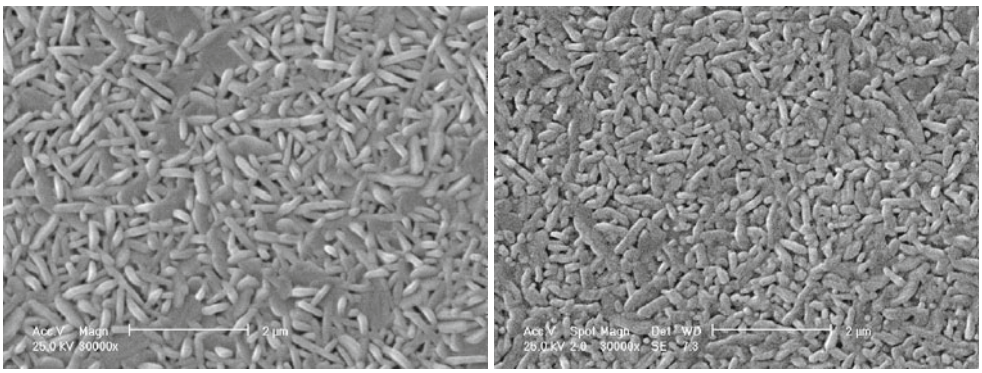

(a) SBTi **(b)** Sr-deficient SBTi

Fig. 2 The SEM images for **a** SBTi and **b** Sr-deficient SBTi thin films

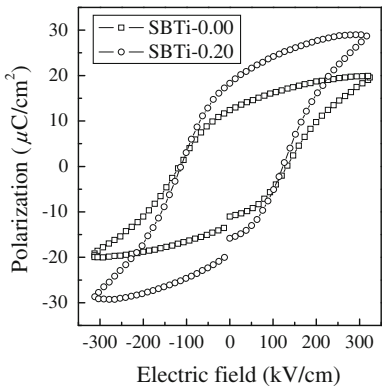

Fig. 3 Hysteresis loops of SBTi and Sr-deficient SBTi films

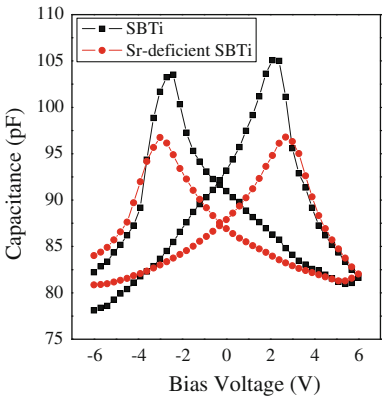

Fig. 4 Variation of capacitance versus voltage for the SBTi and Sr-deficient SBTi films

polymerization, well-controlled pH value during the precursor preparation, the two-step baking and layer-by layer annealing in film crystallization.

The hysteresis behaviors are also reflected in the *C–V* characteristics of both the films, which are shown in Fig. 4. At 100 kHz, the applied voltage was swept from a negative bias to positive bias and back again. Both the films show typical ferroelectric behavior. It is worthy noticed that the Sr-deficient and Bi-excess composition broaden the distance of the two peaks. According to the paper reported by SimÕes et al. [17], it may because that there are some movable ions or charge accumulation at the film-electrode interface, which is pinning the domains. It is reasonable, because the doping of Sr^{2+} by Bi^{3+} may produce some vacancies at A-site.

The enhanced remnant polarization of Sr-deficient and Bi-excess composition will be attributed to the following reasons. First of all, SBTi is a member of BLSFs, and the A-site in the pseudo-perovskite blocks is occupied by Sr^{2+}. Miura and Tanaka [18] examined the substitution of Sr^{2+} by Bi^{3+} at A-site in $Sr_{1-x}Bi_{2+x}Ta_2O_9$ on the basis of an electronic state calculation by the discrete variational *X* method and suggested the possibility that Bi ions occupy the Sr^{2+} site as divalent ions. Shimakawa et al. [19] performed Rietveld analysis for powder neutron diffraction patterns of $Sr_{0.8}Bi_{2.2}Ta_2O_9$, and corroborated the belief that Sr^{2+} is substituted by Bi^{3+} at A-site. Similarly, for SBTi, the substitution of smaller Bi^{3+} ions for Sr^{2+} ions should bring about the vacancies at A-site, cause such compressive stress in the pseudo-perovskite unit to become pronounced [20]. As a result, the lattice mismatch will increase, resulting in the larger distortion in the TiO_6 octahedra and leading to the larger spontaneous polarization. On the other hand, as discussed above, there may be some movable ions in the films, which is pinning the domains. This will decrease the remnant polarization in the SBTi film. In conclusion, the larger P_r of the Sr-deficient SBTi may be the result of both the side competition.

The structural distortion is also related to the ferroelectric Curie temperature [20, 21]. Figure 5 illustrates the temperature dependence of the dielectric constant ε for the stoichiometric and Sr-deficient SBTi ceramics. They show typical ferroelectric behavior with peaks at the Curie temperature T_c. The T_c for stoichiometric SBTi is 520 °C, which coincides with that of reported by Noguchi et al.

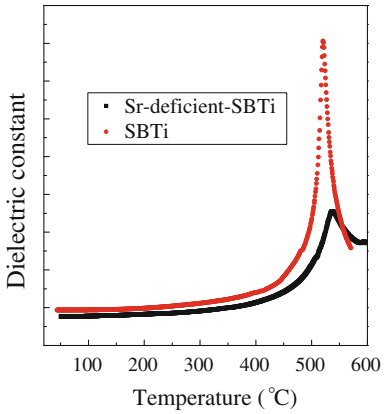

Fig. 5 Dielectric properties of SBTi and Sr-deficient SBTi ceramics

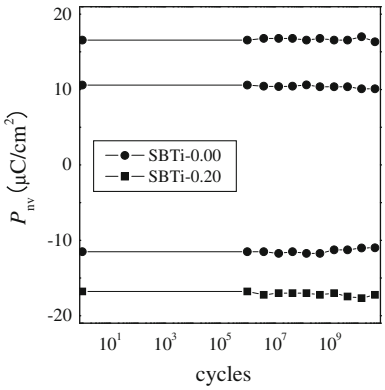

Fig. 6 Fatigue properties of stoichiometric and Sr-deficient SBTi films

[22]. The T_c of Sr-deficient SBTi behaves a slight shift to higher temperature. It may be concluded that the structural distortion increase as the ferroelectric Curie temperature increase.

Fatigue behavior of the SBTi and Sr-deficient-SBTi films were tested using square bipolar pulse at a frequency of 1 MHz and a switching electric field of 200 kV/cm, as shown in Fig. 6. The nonvolatile polarization (P_{nv}) of both the films changes little after 4.4×10^{10} switching cycles. For SBTi film, it might due to the smaller concentration of oxygen vacancy in SBTi thin film, which is derived from the stronger metallicity of strontium than that of bismuth. Moreover, under the same switching pulse, the Sr-deficient–SBTi film shows no fatigue too, suggesting that the substitution of Sr^{2+} by Bi^{3+} does not change the fatigue-free properties of the SBTi films. These are also advantageous for nonvolatile ferroelectric memory applications.

Conclusions

In summary, both stoichiometric SBTi and Sr-deficient SBTi ferroelectric thin films have been deposited on Pt/Ti/SiO_2/Si (100) substrates using the sol–gel process. The films show good ferroelectric properties. The improvement of $2P_r$ induced by the Sr-deficiency and Bi-excess mainly be ascribe to the larger distortion in the TiO_6 octahedra, which is testified by the slight increase of Curie temperature. Moreover, stoichiometric and Sr-deficient SBTi films show fatigue-free characteristics.

References

1. Paz de Araujo CA, Cuchiaro JC, McMillan LD, Scott MC, Scott JF (1995) Nature 374:627
2. Dawber M, Rabe KM, Scott JF (2005) Rev Mod Phys 77:1083
3. Atsuki T, Soyama N, Yonezawa T, Ogi K (1995) Jpn J Appl Phys 34:5096
4. Noguchi T, Hase T, Miyasaka Y (1996) Jpn J Appl Phys 35:4900
5. Noda M, Matsumuro Y, Sugiyama H, Okuyama M (1999) Jpn J Appl Phys 38:2275
6. Cummins SE, Cross LE (1968) J Appl Phys 39:2268
7. Li JJ, Yu J, Li J, Zhou B, Zhou GX, Li YB, Gao JX, Wang YB (2009) J Mater Sci 44:3223. doi:10.1007/s10853-009-3430-y
8. Irie H, Miyayama M (2001) Appl Phys Lett 79:251
9. Zhang ST, Yang B, Chen YF, Liu ZG (2002) J Appl Phys 91:3160
10. Zhang ST, Sun B, Yang B, Chen YF, Liu ZG, Ming NB (2001) Mater Lett 47:334
11. Sohn DS, Xianyu WX, Lee WI, Lee I, Chung I (2001) Appl Phys Lett 79:3672
12. SimÕes AZ, Riccardi CS (2009) Adv Mater Sci Eng 10(1155):928545
13. Do D, Kim SS, Yi SW, Kim JW (2009) Appl Phys A 94:697
14. Wang X, Wang P, Hu CD, Yan J, Chen XM, Ding YX, Wu WB, Fan SH (2008) J Mater Sci Mater Electron 19:1031
15. Ren SB, Lu CJ, Liu JS, Shen HM, Wang YN (1996) Phys Rev B 54:R14337
16. Ren SB, Lu CJ, Shen HM, Wang YN (1997) Phys Rev B 55:3485
17. SimÕes AZ, Ramírez MA, Riccardi CS, Longo E, Varela JA (2005) J Appl Phys 98:114103
18. Miura K, Tanaka M (1998) Jpn J Appl Phys 37:2554
19. Shimakawa Y, Kudo Y, Nakagawa Y, Kamiyama T, Asano H, Izumi F (1999) Appl Phys Lett 74:1904
20. Shimakawa Y, Kubo Y, Tauchi Y, Asano H, Kamiyama T, Iaumi F, Hiroi Z (2001) Jpn J Appl Phys 40:5572
21. Zhu J, Lu WP, Mao XY, Hui R, Chen XB (2003) Jpn J Appl Phys 42:5165
22. Noguchi Y, Miyayama M, Kudo T (2000) Appl Phys Lett 77:3639